

# Open-loop Interconnect Control Schedule Design for Spin Recovery using Direct Numerical Continuation

Rohith G. \* Nandan K. Sinha \*\*

\* *Research Scholar, Department of Aerospace Engineering (e-mail: rohith044@gmail.com).*

\*\* *Professor, Department of Aerospace Engineering (e-mail: nandan@ae.iitm.ac.in)*

*Indian Institute of Technology Madras, Chennai-600036, India*

**Abstract:** Recent interests in Loss-of-Control (LOC) related accidents of aircraft bring back focus on the need for construction of realistic simulations not only of impending accident scenarios but also of recovery of aircraft from fully developed accident scenarios. Developing control schedules for both the activities thereby becomes crucial. In this paper, a novel approach based on constrained numerical continuation procedure is presented to effectively compute open-loop control interconnect schedules for a six-degree-of-freedom aircraft model. For illustrative purposes, the approach based on a new formulation of constraint equations is used to design open-loop control interconnect schedule for recovery of an F-18 HARV model from auto-rotational spin condition.

Copyright © 2020 The Authors. This is an open access article under the CC BY-NC-ND license (<http://creativecommons.org/licenses/by-nc-nd/4.0>)

*Keywords:* Aircraft spin recovery, Bifurcation, Open-loop, Constrained dynamics.

## 1. INTRODUCTION

With increase in air-traffic and unknown factors contributing to aircraft loss-of-control and subsequent accidents, it has become mandatory to train pilots for the unwarranted flight scenarios. Developing control strategies for entry into and recovery from inadvertent flight conditions, thereby, becomes crucial. In order to develop these strategies within the available control authority, both, open-loop control schedules useful for piloted and remote piloted aircraft, and closed-loop control algorithms for aircraft with on-board flight control systems or autonomous systems, are necessary. A special issue dedicated to “Aircraft Loss of Control” published by JGCD (Issue 4, April 2017) calls for a holistic approach to the problem of detecting, preventing, and safely recovering an aircraft either maneuvered into a loss of control scenario or inadvertently trespassing into flight regimes unknown to the pilot (Belcastro et al., 2017; McDonough and Kolmanovsky, 2016; Akametalu et al., 2018; Richards et al., 2016; Kim et al., 2016). Reconstruction of loss of control maneuver for pilot training and devising strategies for recovery both are equally important. In order to design recovery control sequence for aircraft loss-of-control handling, several approaches for fast computation of recoverable sets defined by initial states from which aircraft can be recovered within the control authority available have been presented in (McDonough and Kolmanovsky, 2016). Combining cruise-land phase optimal feedback controller, Akametalu et al. (2018) designed a recovery control sequence for emergency landing of unmanned aerial systems. Richards et al. (2016) proposed an upset recovery-based architecture for designing recovery control sequence for both piloted and unmanned

aircraft. A reinforcement learning based control algorithm has been proposed in (Kim et al., 2016) for recovery of UAVs from undesired conditions. Pilot-Assisted Recovery Systems (PARS) (Paranjape et al., 2017) were recently proposed for energy optimal recovery of aircraft from undesired flight conditions characterized by large flight path angles. While there have been several attempts towards designing closed-loop control algorithms-based recovery strategies (Raghavendra et al., 2005; Sinha and Rao, 2010; Snell et al., 1992), design of open-loop control recovery schedules is inconspicuous.

Open-loop pilot control is intuitive and desired in a normal flight condition. For example, a pilot noticing that aircraft is pitching-up from a cruise flight condition will instinctively apply elevator down or push the stick away to pitch-down the aircraft. While he may get away with undesired development of pitch in this manner, controlling a single degree-of-freedom in motion, in order to counter a simultaneous change in speed from cruise flight condition, he may have to operate both elevator and throttle controls together. Thereby, even in a purely longitudinal flight condition characterized by three degrees of freedom motion, coordination of throttle and elevator or scheduling of throttle and elevator becomes mandatory in order to maintain a particular flight condition in flight. Such open-loop control interconnect schedules can be easily computed by using the constrained bifurcation and continuation procedure first proposed by Ananthkrishnan and Sinha (2001). Using the procedure, design of aileron-rudder-interconnect (ARI) laws for jump prevention in roll maneuver was demonstrated in (Sinha and Ananthkrishnan, 2003). These open-loop control interconnect laws are based on utilizing dynamical system topology to provide a unique way

of charting out a control recovery sequence. Lowenberg (1998) used this route to control spin behavior of a high angle of aircraft model. Scheduling of control parameters based on explicit constraints on states (defining particular flight conditions) and implicit constraints on stability behavior (gain scheduling) exhibit enormous potential of the bifurcation and continuation based techniques (Vora and Sinha, 2017).

Hyper-dimensional topology of a six degree-of-freedom multi-parameter nonlinear aircraft model may provide numerous ways of constructing recovery control sequence. Among the numerous ways, one may find simple, as well as, optimal (energy optimal, time optimal, etc.) control sequences. In this work, usefulness of dynamical system topology is shown in designing control recovery laws for a nonlinear aircraft model. The adopted methodology is based on a constrained continuation procedure outlined in (Vora and Sinha, 2017). In a first, a new formulation of constraints is implemented via aircraft navigational variables in order to compute open-loop control interconnect schedules using the constrained continuation procedure for spin recovery of F-18/HARV model, as an example. Further, numerical time simulation is carried out utilizing the control interconnect schedules to demonstrate the recovery.

The paper is organized as follows. Details of the mathematical model used in this work are presented in Section 2. Section 3 provides adequate description of computation using numerical continuation and the dynamical results for a high angle of attack model of F-18/HARV. Formulation of recovery strategy as a constrained dynamics problem and control interconnect schedules for spin recovery are presented in Section 4. Recovery control sequence and simulation results are presented in Section 5. Conclusions and future directions of work are presented in Section 6.

## 2. MATHEMATICAL MODEL OF AIRCRAFT

The following set of nonlinear ordinary differential equations governing six degree-of-freedom motion of rigid aircraft are used in this work [9].

$$\begin{aligned}\dot{V} &= \frac{1}{m}[\eta T_m \cos\alpha \cos\beta - \bar{q}S(C_D \cos\beta - C_Y \sin\beta) - mg \sin\gamma] \\ \dot{\alpha} &= q - \frac{1}{\cos\beta}[(p \cos\alpha + r \sin\alpha) \sin\beta - \frac{g}{V} \cos\gamma \cos\mu + \frac{\bar{q}S C_L}{mV} \\ &\quad + \frac{\eta T_m \sin\alpha}{mV}] \\ \dot{\beta} &= (p \sin\alpha - r \cos\alpha) + \frac{1}{mV}[-\eta T_m \cos\alpha \sin\beta + \bar{q}S(C_Y \cos\beta \\ &\quad + C_D \sin\beta) + mg \cos\gamma \sin\mu]\end{aligned}\quad (1)$$

$$\begin{aligned}\dot{p} &= \left(\frac{I_y - I_z}{I_x}\right)qr + \frac{1}{I_x}\bar{q}SbC_l \\ \dot{q} &= \left(\frac{I_z - I_x}{I_y}\right)pr + \frac{1}{I_y}\bar{q}S\bar{c}C_m \\ \dot{r} &= \left(\frac{I_x - I_y}{I_z}\right)pq + \frac{1}{I_z}\bar{q}SbC_n\end{aligned}\quad (2)$$

$$\begin{aligned}\dot{\mu} &= \frac{1}{\cos\beta}(p \cos\alpha + r \sin\alpha) + \frac{\bar{q}S C_L}{mV}(\tan\beta + \sin\mu \tan\gamma) \\ &\quad + \frac{\bar{q}S C_Y}{mV} - \frac{g}{V}(\cos\mu \cos\gamma \tan\beta) + \frac{\eta T_m}{mV}[\sin\alpha \tan\beta \\ &\quad + \sin\alpha \sin\mu \tan\gamma - \cos\alpha \sin\beta \cos\mu \tan\gamma] \\ \dot{\gamma} &= \frac{1}{mV}[\eta T_m(\sin\alpha \cos\mu + \cos\alpha \sin\beta \sin\mu) + \bar{q}S C_L \cos\mu \\ &\quad - \bar{q}S C_Y \sin\mu - mg \cos\gamma]\end{aligned}\quad (3)$$

The first set of three equations, Eq. (1), governs the translational motions of a point mass rigid aircraft, the next set of three equations, Eq. (2), governs the angular motions, and Eq. (3) are kinematic equations in windfixed coordinates. The three sets of equations are strongly coupled in a complex six degree-of-freedom motion. Presence of direct nonlinear terms and coupling of various types, viz., aerodynamics, kinematic, geometric, etc. make an aircraft model highly nonlinear (Goman and Khrantsovsky, 1998). The aerodynamic model described by the six coefficients ( $C_L, C_D, C_Y, C_l, C_m, C_n$ ) in the model are dependent on state and control variables of aircraft; the dependencies for the F-18/HARV model used in this work is as given in (Raghavendra et al., 2005).

## 3. HIGH ANGLE-OF-ATTACK SPIN DYNAMICS OF F-18/HARV

In order to investigate global dynamics of a given aircraft model, bifurcation method based techniques can be efficiently utilized. A bifurcation theoretic approach is based on computing steady states of a system of nonlinear ordinary differential equations

$$\dot{\underline{x}} = \underline{f}(\underline{x}, \underline{U}) \quad (4)$$

as function of a varying parameter using a numerical continuation algorithm. For the aircraft model in Eq. (1-3),  $\underline{x} = [V, \alpha, \beta, p, q, r, \mu, \gamma]'$  is the vector of state variables of aircraft,  $\underline{U} = [\eta, \delta e, \delta a, \delta r]'$  is the vector of control parameters, and  $\underline{f}$  is the nonlinear vector field governing aircraft dynamics. Given a starting equilibrium state satisfying

$$\dot{\underline{x}} = \underline{f}(\underline{x}, \underline{U}) = 0, \quad (5)$$

a numerical continuation algorithm solves for connected branches of other equilibrium solutions as function of a varying parameter. Simultaneous computation of local stability of equilibrium states (based on the eigenvalues of Jacobian matrix evaluated at each equilibrium state) and bifurcations (followed by loss of stability at critical equilibrium, marked by one or more eigenvalues lying on the imaginary axis) are unique features of advanced continuation algorithms (Doedel et al., 2007; Dhooge et al., 2003). Further, computation of oscillatory limiting states, their stability, and bifurcations from oscillatory limiting states helps in characterizing global dynamic behavior of a nonlinear aircraft model (Goman and Khrantsovsky, 1998). In order to compute high angle-of-attack spin solutions of the F-18/HARV model, equilibrium solutions of equations of aircraft dynamics (Eq. (1-3)), complete in all respects, are solved as function of elevator deflection, keeping other controls at fixed values. This amounts to solving a set of simultaneous nonlinear algebraic equations (Eq. (1-3) set to zero)

$$\dot{\underline{x}} = \underline{f}(\underline{x}, \delta e, \eta = \text{fixed}, \delta a = 0, \delta r = 0) = 0, \quad (6)$$

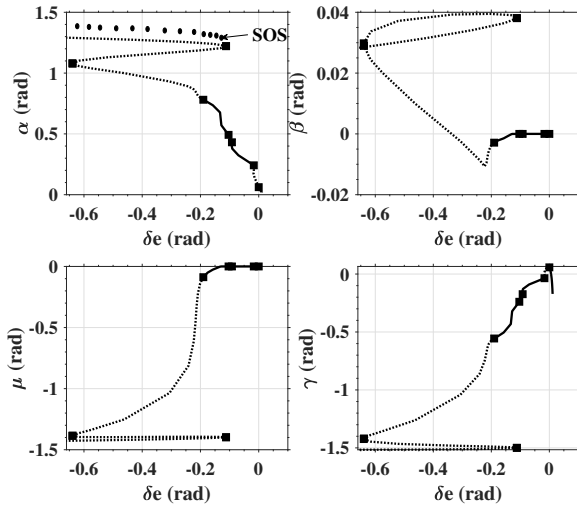


Fig. 1. High angle-of-attack dynamics of F-18/HARV model (Solid lines: stable equilibrium, dashed lines: unstable equilibrium, solid squares: Hopf bifurcations, solid circles: stable oscillatory states).

as function of  $\delta e$ . High angle-of-attack bifurcation results for F-18/HARV model have been presented in various contexts in literature (Raghavendra et al., 2005; Sinha and Rao, 2010; Snell et al., 1992). Nonetheless, for ready reference and for sake of completeness, they are reproduced in Fig. 1 and Fig. 2. Continuation, from a given level flight trim condition (computed otherwise), with elevator deflection varying as continuation parameter computes other connecting branches of equilibrium solutions along with local stability information on the solutions. Reading Fig. 1 from right to left, one can observe that, as elevator up (negative) deflection increases, angle-of-attack increases in a conventional manner. Sideslip angle, roll angle, and rates are zero for up to elevator deflection of about -0.175 rad, indicating, up to this value of elevator deflection, all nominal equilibrium solutions are longitudinal trims. Off-nominal solutions (branching off from nominal solution branch at loss of stability) at low angles of attack resulting from onset of bifurcations and slow departure at moderate to high angles of attack indicate coupled motions in longitudinal and lateral-directional variables.

Post-stall behavior of the F-18/HARV beyond angle-of-attack approximately 0.7 rad corresponding to elevator deflection of about -0.175 rad is dominated by coupled nonlinear motions. The branch of equilibrium solutions of our interest, is corresponding to oscillatory spin states characterized by significantly high yaw rates, and very high angles-of-attack at approximately 1.26 rad (Sinha and Rao, 2010; Rao and Sinha, 2013). Non-zero values of lateral-directional states on this branch indicate that this motion is coupled. Flight path angle on this branch of equilibrium solutions is approximately -1.57 rad characterizing the spin to be ‘flat’ and indicating that aircraft is heading directly vertically down. High negative values of wind-fixed roll angle  $\mu \approx 1.4$  rad indicate a left spin.

It is quite intuitive to understand that a large number of similar two-dimensional curves, for different settings of fixed throttle values and zero aileron and rudder deflec-

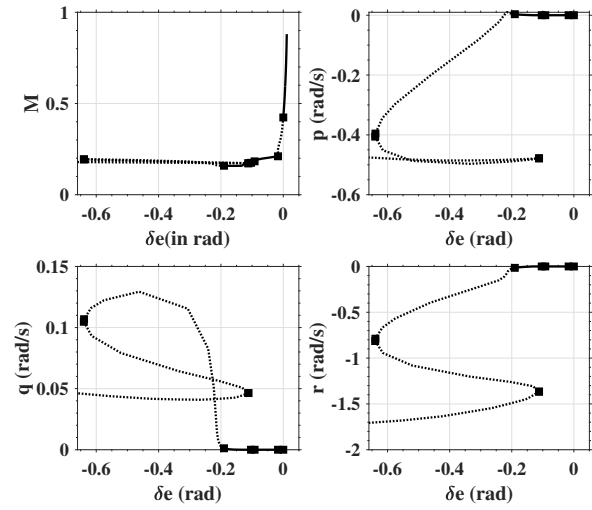


Fig. 2. High angle-of-attack dynamics of F-18/HARV model (Solid lines: stable equilibrium, dashed lines: unstable equilibrium, solid squares: Hopf bifurcations).

tions, can be generated as functions of elevator deflection. Put side-by-side, these curves of equilibrium solutions will constitute a surface for each of the states of aircraft. It becomes not only computationally intensive and time consuming to construct such surfaces that may exhibit folding and unfolding of solution branches, but, it is also difficult to meaningfully visualize these surfaces. Including variations of aileron and rudder deflections, a 4-dimensional topology of each state as function of elevator deflection may emerge, making it further difficult to visualize and analyze the dynamics. Instead, meaningful construction of bifurcation curves utilizing scheduling of control parameters may be more useful in practice. In the following, one such application based control scheduling for spin recovery is presented.

#### 4. COMPUTATION OF CONTROL INTERCONNECT SCHEDULES FOR SPIN RECOVERY

There has been a lot of work on designing closed-loop control laws for aircraft recovery from spin, extremely important for autonomous aircraft and aircraft with on-board control systems. Prominent among them being spin recovery control design using sliding mode and nonlinear dynamic inversion based control techniques (Raghavendra et al., 2005; Sinha and Rao, 2010; Snell et al., 1992) and, more recently, one based on reinforced learning based control (Kim et al., 2016). However, there has not been any visible attempt towards designing recovery laws for pilot operated aircraft. A method based on constrained continuation procedure (Lowenberg, 1998) is adopted here to compute open-loop control interconnect schedule for spin recovery. In a constrained continuation, computation of steady state solutions of Eq. (1) augmented with equality constraint equations

$$\dot{\underline{x}} = \underline{f}(\underline{x}, \underline{U}); \underline{g}(\underline{x}, \underline{U}) = 0 \quad (7)$$

is carried out. The steady state solution thus computed are not ordinary but the ones that satisfy the constraints,

$$\underline{g}(\underline{x}, \underline{U}) = 0. \quad (8)$$

The control schedules (variations of control parameters  $p \in \underline{U}$  as function of continuation parameter) required to satisfy the constraints are also computed in this manner. Several examples of this increased functionality of continuation techniques have been presented in (Spetzler and Narang-Siddarth, 2016) and more recently in (Vora and Sinha, 2017). The examples show unique capabilities of a numerical continuation algorithm in solving  $n$  coupled nonlinear algebraic equations in  $n + 1$  unknowns, where one of the unknowns is the varying continuation parameter. Extending the work, here, a new formulation is presented for the constraint equations so as to define a recovery procedure from an auto-rotational spin condition. Except for the procedure outlined in flight manuals (ICAO, 2014) which was used to design a trial and error based recovery procedure for F-18 from spin in (Rao and Sinha, 2013), there exists no proper procedure to directly compute control interconnect schedules for airplane recovery from undesired flight conditions. Autorotational spin solutions computed in Fig. 1 corresponds to fixed value of throttle, and neutral aileron and rudder deflections, which are pure consequence of high angle-of-attack aerodynamics. Nullifying the aerodynamic effects using elevator alone to bring back the angle-of-attack to a pre-stall stable cruise flight condition may appear intuitive, but the ensuing motion in a spin is a coupled nonlinear motion and, thereby, requires appropriate use of non-longitudinal control inputs as well. Closed-loop spin recovery presented in (Kim et al., 2016; Raghavendra et al., 2005; Sinha and Rao, 2010) suggests use of all available control inputs simultaneously. While throttle input is also auto-computed as closed-loop control along with elevator, rudder, aileron deflections in (Kim et al., 2016), in (Raghavendra et al., 2005; Sinha and Rao, 2010), throttle is used in open-loop as first order input. In the following open-loop control interconnect schedule computation, all available control inputs are computed together as function of elevator deflection.

The novel approach is based on using triplet of angles  $(\gamma, \beta, \mu)$  as representative of any current (un-desired) and intended (desired) flight conditions. For example, in autorotational spin condition one can read the values of these angles from Fig. 1 as  $(\gamma \approx -1.57\text{rad}, \beta \approx 0.028\text{rad}, \mu \approx -1.4\text{rad})$ . The intended state, a cruise flight condition, in terms of values of these angles is given by  $(\gamma \approx 0\text{rad}, \beta \approx 0\text{rad}, \mu \approx 0\text{rad})$ . In addition, the intended flight condition (to which aircraft needs to recover) has to be stable. This is a deviation from the desired state defined in term of exact values of  $(\gamma, \beta, \mu)$  representing a unique cruise flight condition used in (Rao and Sinha, 2013) for computing the spin recovery controls. Constraints are formulated now as curves joining the two states in the following manner:

$$\gamma - g_1(\delta e) = 0; \beta - g_2(\delta e) = 0; \mu - g_3(\delta e) = 0 \quad (9)$$

owing to the requirement that remaining control inputs are to be scheduled as function of the elevator deflection, which is to be used as the continuation parameter. It must be obvious that there are infinitely many ways in which the functions  $g_1, g_2$  and  $g_3$  can be generated, the other concern being that these functions must be smooth. The smoothness criterion required for continuation demands that functions must be continuous and differentiable (Goman and Khramtsovsky, 1998). While a rigorous presentation covering all aspects of this approach may be much

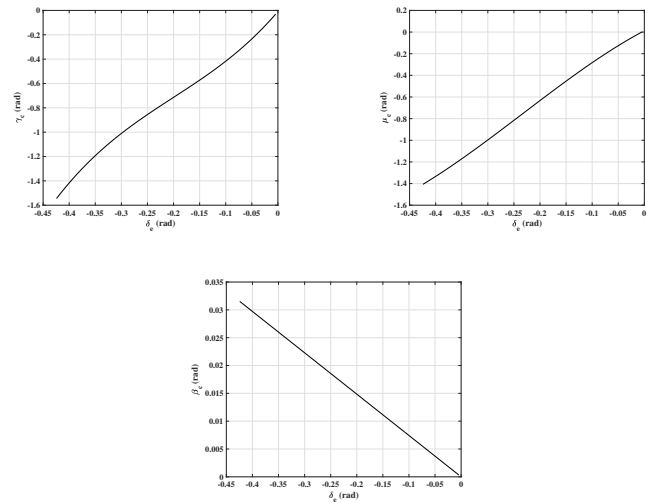


Fig. 3.  $\gamma, \mu$  and  $\beta$  profiles for spin recovery.

desired, the primary objective of this work is to showcase usefulness of this approach. In the following, these functions are selected as shown in Fig. 3.  $g_1, g_3$  are selected as quadratic functions and,  $g_2$  chosen to be a linear function of  $\delta e$ .

The constraints in Eq. (9) are coupled with the available controls, throttle, rudder and aileron, respectively, and are, therefore, achievable (Ananthkrishnan and Sinha, 2001). Therefore, these controls are left free to vary in a continuation in order to account for the additional three constraint Eq. (9) added to original eight equations of aircraft motion (Eq. (1-3)). Solving simultaneous 11 equations (Eqs. (1-3) set to zero and Eq. (9)) for aircraft equilibrium states satisfying the constraints results in schedules of the freed controls as function of the varying control parameter, elevator deflection. Simultaneous computation of stability of the constrained equilibrium states are automated using the procedure outlined in (Lowenberg, 1998).

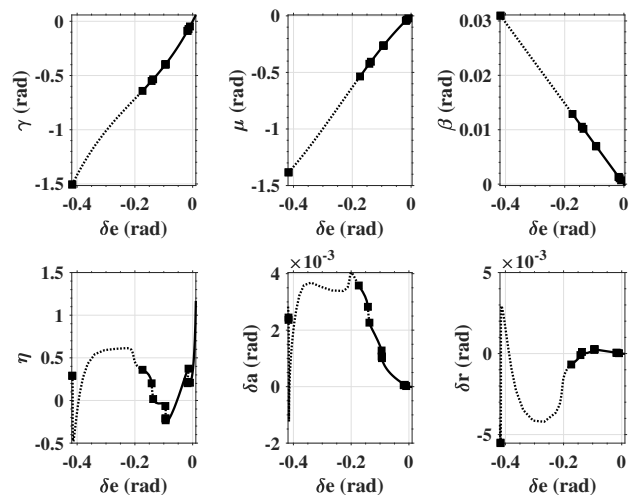


Fig. 4. Bifurcation plot of constrained variables and control interconnect schedules as functions of  $\delta e$  (Solid lines: stable equilibrium, dashed lines: unstable equilibrium, solid squares: Hopf bifurcations).

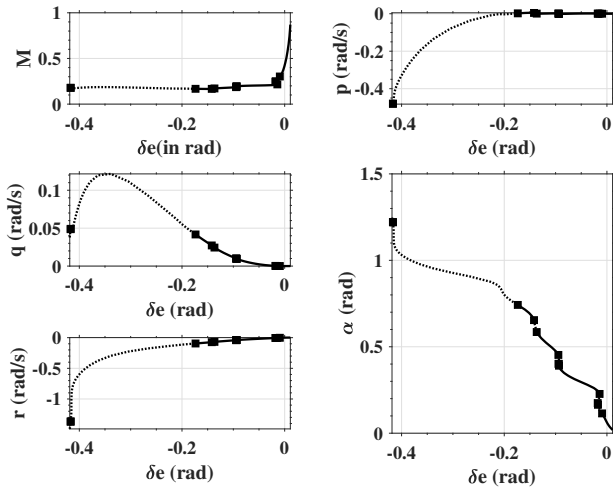


Fig. 5. Other states as function of  $\delta_e$  (Solid lines: stable equilibrium, dashed lines: unstable equilibrium, solid squares: Hopf bifurcations).

Continuation results of this computation are presented in Fig. 4. Top row plots in Fig. 4 shows variation of the constrained variables as functions of the elevator deflection, which are same as the desired variations (shown in Fig. 3), but with stability and bifurcations marked on them. These results indicate that not all intermediate equilibrium states are stable. Also shown along in Fig. 4 (bottom row plots) are the computed control interconnect schedules required to achieve the constraints on  $(\gamma, \beta, \mu)$  as per the constraints, which will be later used for designing recovery sequence. For aerodynamic benefits, the control inputs are required to be within the limits as prescribed in Raghavendra et al. (2005). Throttle fraction in excess of maximum ‘1’ can be avoided. Figure 4 shows variation of other states as function of elevator deflection  $\delta_e$  as simple curves projected in 2-dimension.

### 5. RESULTS AND DISCUSSIONS

Figure 4 (bottom row) presents unique plots that can be used to design control inputs in numerous ways to recover the aircraft from spin. The pilot control inputs thus can be organized appropriately providing the desired recovery strategy. The constraints curves for  $(\gamma, \beta, \mu)$  connect the spin solution to level flight condition ( $\gamma \approx 0rad, \beta \approx 0rad, \mu \approx 0rad$ ) at the right top corner in Fig. 4, which is the desired state and is stable. Corresponding values for other states defining the level flight equilibrium state can be read from Fig. 5. Intermediate equilibrium states can be utilized for hopping between the states while satisfying the rate and position constraints on the control inputs. This procedure allows various profiles of control recovery commands, which may, for example, be based on handling and flight qualities of aircraft and/or accounting for spatial disorientation that pilots may be undergoing in this complex motion.

In order to show the efficacy of this approach, time histories of control inputs are defined arbitrarily as shown in Fig. 6. The control schedules computed in Fig. 4 correspond to steady states; in-between time histories of other control inputs can be directly defined as following

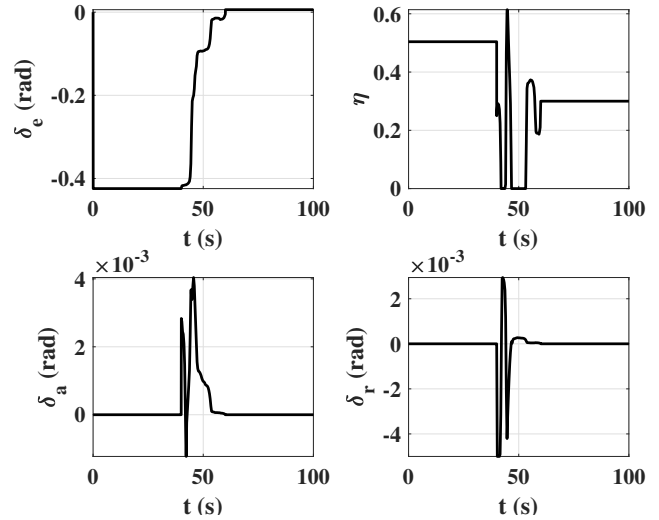


Fig. 6. Control input histories based on open loop schedules in Fig. 4.

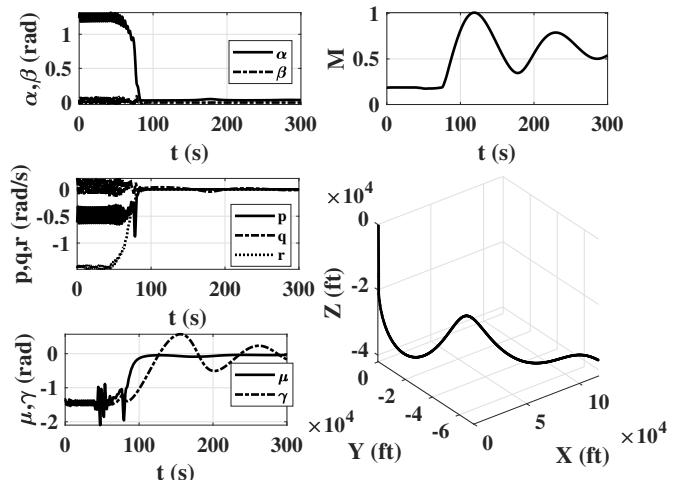


Fig. 7. Time simulation results for the open loop control inputs in Fig. 6 for spin recovery.

elevator input time history as per schedules, or, they can be independently defined between their steady state values as per Fig. 4. In the simulation, we chose throttle, aileron, and rudder control commands to follow elevator input command history as shown in Fig. 6. In Fig.7, spin recovery simulation results are presented for control inputs in Fig. 6. The recovery control sequence is activated at 40 seconds when the aircraft is in fully developed oscillatory spin state. Recovery from spin to level flight condition at a low angle-of-attack equilibrium state can be observed from Fig. 7. Interestingly, these results are very similar to the results for closed-loop spin recovery presented earlier in (Raghavendra et al., 2005; Khatri et al., 2012), thus, establishing the role of continuation based dynamic analysis and usefulness of dynamical system topology for recovery control design. The altitude drop during the recovery is also in the same range as presented in previous works. For aircraft not equipped with on-board flight control systems, open loop recovery strategies are very useful. Moreover, most of the conventional autopilot systems are designed for nominal conditions which disengage if situation goes

erratic, and in such scenarios, initiating open-loop recovery may be the only option available.

## 6. CONCLUSIONS

In this work, a new formulation based on constraints on navigation variables has been presented for computing control interconnect schedules to construct recovery maneuver for aircraft. For illustration, spin recovery control sequence is generated for the F-18/HARV model from the control interconnect schedules computed using the bifurcation and continuation technique. Computation of such schedules based on constraints on navigational variables provides a unique way of designing control recovery sequence within the available control limits. This approach can be employed for better equipping/training pilots to address loss of control scenarios in real-life situations. It is interesting to note that, there are many ways in which the constraint functions can be formulated. How to select the constraint functions so as to design control recovery sequence with optimality requirements could be a possible future direction of this work.

## REFERENCES

- Akametalu, A.K., Tomlin, C.J., and Chen, M. (2018). Reachability-based forced landing system. *Journal of Guidance, Control, and Dynamics*, 41(12), 2529–2542.
- Ananthkrishnan, N. and Sinha, N.K. (2001). Level flight trim and stability analysis using extended bifurcation and continuation procedure. *Journal of Guidance, Control, and Dynamics*, 24(6), 1225–1228.
- Belcastro, C.M., Foster, J.V., Shah, G.H., Gregory, I.M., Cox, D.E., Crider, D.A., Groff, L., Newman, R.L., and Klyde, D.H. (2017). Aircraft loss of control problem analysis and research toward a holistic solution. *Journal of Guidance, Control, and Dynamics*, 40(4), 733–775.
- Dhooge, A., Govaerts, W., and Kuznetsov, Y.A. (2003). Matcont: a matlab package for numerical bifurcation analysis of odes. *ACM Transactions on Mathematical Software (TOMS)*, 29(2), 141–164.
- Doedel, E.J., Champneys, A.R., Dercole, F., Fairgrieve, T., Yu, A., Oldeman, B., Paffenroth, R., Sandstede, B., Wang, X., Zhang, C., et al. (2007). Auto-07p: Continuation and bifurcation software for ordinary differential equations. Technical report.
- Goman, M. and Khramtsovsky, A. (1998). Application of continuation and bifurcation methods to the design of control systems. *Philosophical Transactions of the Royal Society of London. Series A: Mathematical, Physical and Engineering Sciences*, 356(1745), 2277–2295.
- ICAO (2014). Manual of Aeroplane Upset Prevention and Recovery Training, Doc.10011 AN/506. Technical report, International Civil Aviation Organization.
- Khatri, A.K., Singh, J., and Sinha, N.K. (2012). Aircraft maneuver design using bifurcation analysis and sliding mode control techniques. *Journal of Guidance, Control, and Dynamics*, 35(5), 1435–1449.
- Kim, D., Oh, G., Seo, Y., and Kim, Y. (2016). Reinforcement learning-based optimal flat spin recovery for unmanned aerial vehicle. *Journal of Guidance, Control, and Dynamics*, 40(4), 1076–1084.
- Lowenberg, M. (1998). Development of control schedules to modify spin behaviour. In *23rd Atmospheric Flight Mechanics Conference*, 4267. Boston, Massachusetts.
- McDonough, K. and Kolmanovsky, I. (2016). Fast computable recoverable sets and their use for aircraft loss-of-control handling. *Journal of Guidance, Control, and Dynamics*, 40(4), 934–947.
- Paranjape, A.A., Dama, S., Abhilash, P., and Sura, N.K. (2017). Optimization and analysis of a pilot-activated automatic recovery system. *Journal of Aircraft*, 55(2), 841–852.
- Raghavendra, P., Sahai, T., Kumar, P.A., Chauhan, M., and Ananthkrishnan, N. (2005). Aircraft spin recovery, with and without thrust vectoring, using nonlinear dynamic inversion. *Journal of Aircraft*, 42(6), 1492–1503.
- Rao, D.M.K.K.V. and Sinha, N.K. (2013). A sliding mode controller for aircraft simulated entry into spin. *Aerospace Science and Technology*, 28(1), 154–163.
- Richards, N.D., Gandhi, N., Bateman, A.J., Klyde, D.H., and Lampton, A.K. (2016). Vehicle upset detection and recovery for onboard guidance and control. *Journal of Guidance, Control, and Dynamics*, 40(4), 920–933.
- Sinha, N.K. and Rao, D.M.K.K.V. (2010). Aircraft spin recovery using a sliding-mode controller. *Journal of guidance, control, and dynamics*, 33(5), 1675–1679.
- Sinha, N. and Ananthkrishnan, N. (2003). Bifurcation analysis of inertia coupled roll manoeuvres of airplanes. *Proceedings of the Institution of Mechanical Engineers, Part G: Journal of Aerospace Engineering*, 217(2), 75–85.
- Snell, S.A., Nns, D.F., and Arrard, W.L. (1992). Nonlinear inversion flight control for a supermaneuverable aircraft. *Journal of guidance, control, and dynamics*, 15(4), 976–984.
- Spetzler, M.G. and Narang-Siddarth, A. (2016). Increased functionality of continuation-based nonlinear system analysis. *Journal of Guidance, Control, and Dynamics*, 1206–1222.
- Vora, A.S. and Sinha, N.K. (2017). Direct methodology for constrained system analysis with applications to aircraft dynamics. *Journal of Aircraft*, 54(6), 2378–2385.

## NOMENCLATURE

$M$	Mach Number
$\alpha$	Angle of attack
$\beta$	Sideslip angle
$p, q, r$	Body axis roll, pitch and yaw rates, respectively
$\mu, \gamma$	Bank angle and flight path angle, respectively
$X, Y, Z$	Position coordinates
$T$	Thrust
$T_m$	Maximum thrust
$\eta$	Thrust as a fraction of max. available thrust
$\delta e$	Elevator deflection,
$\delta a$	Aileron deflection,
$\delta r$	Rudder deflection,
$C_L, C_D$	Lift and drag coefficients, respectively
$C_m$	Aerodynamic pitching moment coefficient
$C_l, C_n$	Aerodynamic rolling moment coefficient
$C_l, C_n$	Aerodynamic yawing moment coefficient
$C_Y$	Coefficient of sideforce